

Most charming dibaryon near unitarity

Yan Lyu,^{1,2,*} Hui Tong,^{1,3,†} Takuya Sugiura,³ Sinya Aoki,^{4,2}
Takumi Doi,^{2,3} Tetsuo Hatsuda,³ Jie Meng,^{1,5} and Takaya Miyamoto²

¹State Key Laboratory of Nuclear Physics and Technology,
School of Physics, Peking University, Beijing 100871, China

²Quantum Hadron Physics Laboratory, RIKEN Nishina Center, Wako 351-0198, Japan

³Interdisciplinary Theoretical and Mathematical Sciences Program (iTHEMS), RIKEN, Wako 351-0198, Japan

⁴Center for Gravitational Physics, Yukawa Institute for Theoretical Physics, Kyoto University, Kyoto 606-8502, Japan

⁵Yukawa Institute for Theoretical Physics, Kyoto University, Kyoto 606-8502, Japan

A pair of triply charmed baryons, $\Omega_{ccc}\Omega_{ccc}$, is studied as an ideal dibaryon system by (2+1)-flavor lattice QCD with nearly physical light-quark masses and the relativistic heavy quark action with the physical charm quark mass. The spatial baryon-baryon correlation is related to their scattering parameters on the basis of the HAL QCD method. The $\Omega_{ccc}\Omega_{ccc}$ in the 1S_0 channel taking into account the Coulomb repulsion with the charge form factor of Ω_{ccc} leads to the scattering length $a_0^C \simeq -19$ fm and the effective range $r_{\text{eff}}^C \simeq 0.45$ fm. The ratio $r_{\text{eff}}^C/a_0^C \simeq -0.024$, whose magnitude is considerably smaller than that of the dineutron (-0.149), indicates that $\Omega_{ccc}\Omega_{ccc}$ is located in the unitary regime.

Introduction.— Quantum chromodynamics (QCD) is a fundamental theory of strong interaction and governs not only the interaction among quarks and gluons but also the interaction between color-neutral hadrons. In particular, the nucleon-nucleon (NN) interaction, which shows a characteristic mid-range attraction and a short-range repulsion, as well as the baryon-baryon (BB) interactions are important for describing the nuclear structure and dense matter relevant to nuclear physics and astrophysics [1–5].

Although the deuteron is the only stable bound state composed of two nucleons, there are possible bound or resonant dibaryons with and without strange quarks [6–8]. Among others, $p\Omega(uudsss)$ [9] and $\Omega\Omega(ssssss)$ [10], which were predicted by lattice QCD (LQCD) simulations near the physical point [11], stimulate experimental searches in high energy hadron-hadron and heavy-ion collisions [8, 12–14].

As originally pointed out by Bjorken [15], the triply charmed baryon (the charm number $C = 3$) Ω_{ccc} is stable against the strong interaction and provides an ideal ground to study the perturbative and non-perturbative aspects of QCD in the baryonic sector. Although it has not been observed yet experimentally¹ there have been numerous LQCD studies on its mass and electromagnetic form factor (see [18] and references therein). Accordingly, it is timely to study the $\Omega_{ccc}\Omega_{ccc}$ as the simplest possible system to study heavy-baryon interactions. Its recent phenomenological study using the constituent quark model can be found in Ref. [19].

The purpose of this Letter is to study a system with the charm number $C = 6$ system, $\Omega_{ccc}\Omega_{ccc}$ in the 1S_0 channel, for the first time from first principle LQCD ap-

proach.² The reason why we consider the S -wave and total spin $s = 0$ system is that the Pauli exclusion between charm quarks at short distance does not operate in this channel, so that the maximum attraction is expected in comparison to other channels. It is of critical importance to examine the scattering parameters such as the scattering length and the effective range to unravel the properties of such heavy dibaryons near threshold. The HAL QCD method [11, 22, 23], which treats the spatial correlation between two baryons on the lattice, provides a powerful tool for such analysis: Indeed, we show below that $\Omega_{ccc}^{++}\Omega_{ccc}^{++}(^1S_0)$ with both strong interaction and Coulomb repulsion is located near unitarity [24, 25] just above the threshold with a large negative scattering length.

HAL QCD Method.— The crucial steps in the HAL QCD method [11, 22, 23] are to obtain the equal-time Nambu-Bethe-Salpeter (NBS) wave function $\psi(\mathbf{r})$ whose asymptotic behavior at a large distance reproduces the phase shifts, along with the corresponding two-baryon irreducible kernel $U(\mathbf{r}, \mathbf{r}')$. Since the same kernel $U(\mathbf{r}, \mathbf{r}')$ governs all the elastic scattering states, separating the ground state and the excited states on the lattice, which is exponentially difficult for baryon-baryon interactions [26, 27], is not required to calculate the physical observables [23]. The normalized four-point function (the R -correlator) related to the NBS wave function is defined as

$$\begin{aligned} R(\mathbf{r}, t > 0) &= \langle 0 | \Omega_{ccc}(\mathbf{r}, t) \Omega_{ccc}(\mathbf{0}, t) \bar{\mathcal{J}}(0) | 0 \rangle / e^{-2m_{\Omega_{ccc}} t} \\ &= \sum_n A_n \psi_n(\mathbf{r}) e^{-(\Delta W_n)t} + O(e^{-(\Delta E^*)t}), \end{aligned} \quad (1)$$

¹ Recently, excited states of $C = 1$ baryon Ω_c [16] and a $C = 2$ baryon Ξ_{cc}^{++} [17] were discovered at CERN LHC.

² In the charm number $C = 3$ sector, there exist a few recent studies on heavy dibaryons in LQCD [20] and in the constituent quark model [21].

where $\Delta W_n = 2\sqrt{m_{\Omega_{ccc}}^2 + \mathbf{k}_n^2} - 2m_{\Omega_{ccc}}$ with the baryon mass $m_{\Omega_{ccc}}$ and the relative momentum \mathbf{k}_n . $O(e^{-(\Delta E^*)t})$ denotes the contributions from the inelastic scattering states with ΔE^* being the inelastic threshold, which are exponentially suppressed when $t \gg (\Delta E^*)^{-1} \sim \Lambda_{\text{QCD}}^{-1}$ with $\Lambda_{\text{QCD}} \sim 300$ MeV. $\bar{\mathcal{T}}(0)$ is a source operator which creates two-baryon states with the charm number $C = 6$ at Euclidean time $t = 0$ and $A_n = \langle n | \bar{\mathcal{T}}(0) | 0 \rangle$ with $|n\rangle$ representing the QCD eigenstates in a finite volume with $\Delta W_n < \Delta E^*$. In this study, we take a local interpolating operator, $\Omega_{ccc}(x) \equiv \epsilon^{lmn} [c_l^T(x) \mathcal{C} \gamma_k c_m(x)] c_{n,\alpha}(x)$, where l, m , and n stand for color indices, γ_k being the Dirac matrix, α being the spinor index, and $\mathcal{C} \equiv \gamma_4 \gamma_2$ being the charge conjugation matrix.

When contributions from the inelastic scattering states are negligible ($t \gg (\Delta E^*)^{-1}$), the R -correlator satisfies [23]

$$\left(\frac{1}{4m_{\Omega_{ccc}}} \frac{\partial^2}{\partial t^2} - \frac{\partial}{\partial t} - H_0 \right) R(\mathbf{r}, t) = \int d\mathbf{r}' U(\mathbf{r}, \mathbf{r}') R(\mathbf{r}', t), \quad (2)$$

where $H_0 = -\nabla^2/m_{\Omega_{ccc}}$. By using the derivative expansion at low energies, $U(\mathbf{r}, \mathbf{r}') = V(r)\delta(\mathbf{r} - \mathbf{r}') + \sum_{n=1} V_{2n}(\mathbf{r}) \nabla^{2n} \delta(\mathbf{r} - \mathbf{r}')$, the central potential $V(r)$ in the leading order (LO) is given as

$$V(r) = R^{-1}(\mathbf{r}, t) \left(\frac{1}{4m_{\Omega_{ccc}}} \frac{\partial^2}{\partial t^2} - \frac{\partial}{\partial t} - H_0 \right) R(\mathbf{r}, t). \quad (3)$$

The spatial and temporal derivatives of $R(\mathbf{r}, t)$ on the lattice are calculated in central difference scheme by using the nearest neighbor points. To extract the total spin $s = 0$, the following interpolating operators for the $\Omega_{ccc}\Omega_{ccc}$ system is adopted, $[\Omega_{ccc}\Omega_{ccc}]_0 = \frac{1}{2}(\Omega_{ccc}^{3/2}\Omega_{ccc}^{-3/2} - \Omega_{ccc}^{1/2}\Omega_{ccc}^{-1/2} + \Omega_{ccc}^{-1/2}\Omega_{ccc}^{1/2} - \Omega_{ccc}^{-3/2}\Omega_{ccc}^{3/2})$. Here the spin and its z component of the interpolating operator $\Omega_{ccc}^{s_z}$ are $3/2$ and $s_z = \pm 3/2, \pm 1/2$, respectively, and $\Omega_{ccc}^{s_z}$ is constructed by spin projection as shown in Ref. [28]. To obtain the orbital angular momentum $L = 0$ on the lattice, the projection to A_1 representation of the cubic group $SO(3, \mathbf{Z})$ is employed; $P^{A_1} R(\mathbf{r}, t) = \frac{1}{24} \sum_{\mathcal{R}_i \in SO(3, \mathbf{Z})} R(\mathcal{R}_i[\mathbf{r}], t)$.

Lattice setup.— (2+1)-flavor gauge configurations are generated on the $L^4 = 96^4$ lattice with the Iwasaki gauge action at $\beta = 1.82$ and nonperturbatively $O(a)$ -improved Wilson quark action combined with stout smearing at nearly physical quark masses ($m_\pi \simeq 146$ MeV and $m_K \simeq 525$ MeV) [29]. The lattice cutoff is $a^{-1} \simeq 2.333$ GeV ($a \simeq 0.0846$ fm), corresponding to $La \simeq 8.1$ fm, which is sufficiently large to accommodate two heavy baryons. For the charm quark, we employ the relativistic heavy quark (RHQ) action in order to remove the leading order and the next-to-leading order cutoff errors associated with the charm quark mass [30]. We use two sets (set 1 and set 2) of RHQ parameters determined in Ref. [31] so

as to interpolate the physical charm quark mass and reproduce the dispersion relation for the spin-averaged $1S$ charmonium, i.e. a weighted average of the spin-singlet state η_c and the spin-triplet state J/Ψ .

For the source operator $\bar{\mathcal{T}}(0)$, we use the wall type with the Coulomb gauge fixing. We employ the periodic (Dirichlet) boundary condition for spatial (temporal) direction. We use 112 gauge configurations which are picked up one per ten trajectories. In order to reduce statistical fluctuations, forward and backward propagations are averaged, and four times measurements are performed by shifting source position along the temporal direction for each configuration. Then, the total measurements amount to 896 for each set. The statistical errors are estimated by the jackknife method with a bin size of 14 configurations. A comparison with a bin size of 7 configurations shows that the bin size dependence is small. The quark propagators are calculated by the Bridge++ code [32], and the unified contraction algorithm is utilized to obtain the correlation functions [33].

TABLE I. Spin-averaged $1S$ charmonium mass ($(m_{\eta_c} + 3m_{J/\Psi})/4$) and the Ω_{ccc} mass ($m_{\Omega_{ccc}}$) calculated in set 1 and set 2 with the statistical errors. The third row shows the interpolated values obtained from set 1 and set 2. Experimental value of $(m_{\eta_c} + 3m_{J/\Psi})/4$ is shown in the last row.

	$(m_{\eta_c} + 3m_{J/\Psi})/4$ [MeV]	$m_{\Omega_{ccc}}$ [MeV]
set 1	3096.6(0.3)	4837.3(0.7)
set 2	3051.4(0.3)	4770.2(0.7)
Interpolation	3068.5(0.3)	4795.6(0.7)
Exp.	3068.5(0.1)	-

Masses for spin-averaged $1S$ charmonium ($(m_{\eta_c} + 3m_{J/\Psi})/4$) and Ω_{ccc} baryon ($m_{\Omega_{ccc}}$) calculated in set 1 and set 2 by utilizing the single exponential fitting from the interval $t/a = 25 - 35$ are listed in Table. I, together with the values from linear interpolation ($0.3786 \times \text{set 1} + 0.6214 \times \text{set 2}$) as well as the experimental value. Our result for $m_{\Omega_{ccc}}$ is consistent with 4789(6)(21) MeV obtained by the (2+1)-flavor PACS-CS configurations [34]. We have checked that our results for hadron masses are unchanged within errors by the fitting interval $t/a = 30 - 35$.

Numerical results.— The $\Omega_{ccc}\Omega_{ccc}$ potential $V(r)$ in the 1S_0 channel from the interpolation between set 1 and set 2 is shown in Fig. 1 for $t/a = 25, 26$ and 27 . Since the potentials from set 1 and set 2 are found to be consistent within statistical errors, the uncertainty in the interpolation is negligible. Our choice $t/a = 26$ corresponds to $t \simeq 2.2$ fm; this is large enough in comparison to the typical length scale $\Lambda_{\text{QCD}}^{-1} \sim 0.7$ fm characterizing the inelastic states, and is small enough to avoid large statistical errors. We find that the potentials for $t/a = 25, 26$ and 27 are consistent with each other within statistical errors. This indicates that systematic errors due to inelastic states and higher order terms of the deriva-

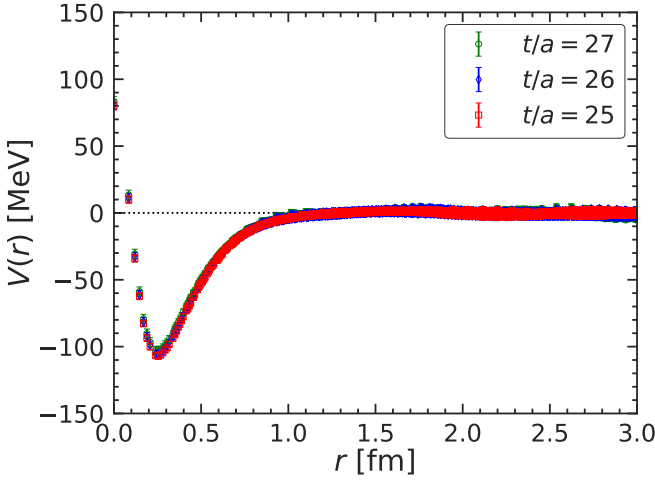


FIG. 1. (Color online). The $\Omega_{ccc}\Omega_{ccc}$ potential $V(r)$ in the 1S_0 channel as a function of separation r at Euclidean time $t/a = 25$ (red square), 26 (blue diamond) and 27 (green circle).

tive expansion do not largely exceed the size of statistical errors [23] as we show below.

We find that the potential $V(r)$ is repulsive at short-range and attractive at mid-range, which has the same qualitative behaviors with the NN potential [35] and the $\Omega\Omega$ potential [10]. The magnitude of the potential in the repulsive region $r < 0.25$ fm (corresponding to $dV(r)/dr < 0$) for $\Omega_{ccc}\Omega_{ccc}$ is an order of magnitude smaller than that of $\Omega\Omega$ obtained by the same method [10]. This may be qualitatively explained by the phenomenological quark model [36] as the color-magnetic interaction between constituent quarks is proportional to the square of reciprocal constituent quark mass. Qualitatively, $V_{cm}^{cc}/V_{cm}^{ss} = (m_s^*/m_c^*)^2 \sim (500/1500)^2 \sim 0.1$, where $V_{cm}^{ff'}$ is the color-magnetic interaction between the quarks with flavor f and f' with m_f^* being the constituent quark mass. On the other hand, the attraction in the region $r > 0.25$ fm (corresponding to $dV(r)/dr > 0$) may originate from the exchange of charmed mesons or rather be attributed to the direct exchange of charm quarks and/or multiple gluons. As can be seen in Fig. 1, the range of the potential is much smaller than the size of the lattice volume, indicating that the finite volume artifact is negligible.

In order to convert the potential to physical observables such as the scattering phase shifts and binding energy, we perform the uncorrelated fit for $V(r)$ in Fig. 1 in the range $r \leq 2.5$ fm by three-range Gaussians, $V_{fit}(r) = \sum_{i=1,2,3} \alpha_i \exp(-\beta_i r^2)$. Fitting parameters with $t/a = 26$ for example are $(\alpha_1, \alpha_2, \alpha_3) = (239.5(3.0), -62.7(50.8), -98.8(50.3))$ in MeV and $(\beta_1, \beta_2, \beta_3) = (48.5(1.4), 7.8(2.6), 3.4(0.8))$ in fm^{-2} with an accuracy of $\chi^2/\text{d.o.f.} \sim 1.05$.

In Fig. 2, we show the $\Omega_{ccc}\Omega_{ccc}$ scattering phase

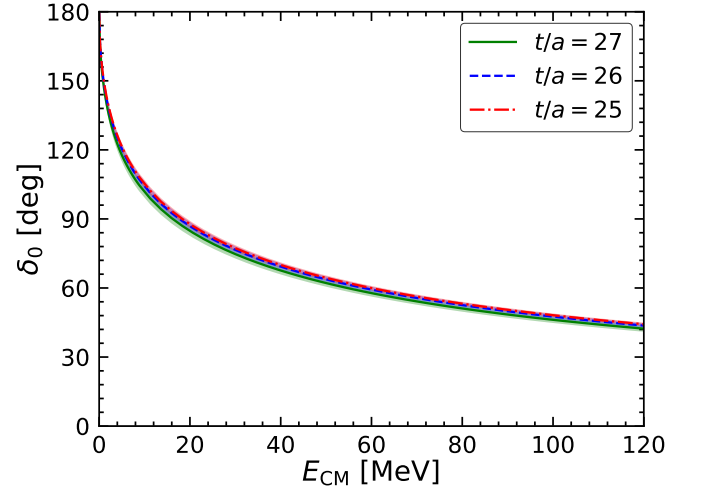


FIG. 2. (Color online). The $\Omega_{ccc}\Omega_{ccc}$ scattering phase shifts δ_0 in the 1S_0 channel obtained from the potential $V(r)$ at $t/a = 25, 26$, and 27 as a function of the center of mass kinetic energy E_{CM} .

shifts δ_0 in the 1S_0 channel calculated by solving the Schrödinger equation with the potential $V(r)$ at $t/a = 25, 26$, and 27. The relativistic kinetic energy is defined as $E_{CM} = 2\sqrt{k^2 + m_{\Omega_{ccc}}^2} - 2m_{\Omega_{ccc}}$ with a momentum k in the center of mass frame. The error bands reflect the statistical uncertainty of $V(r)$. In all three cases, the phase shifts start from 180° at $E_{CM} = 0$, which indicates the existence of a bound state in $\Omega_{ccc}\Omega_{ccc}$ system without Coulomb repulsion.

The low-energy scattering parameters are extracted by using the effective range expansion up to the next-to-leading order (NLO), $k \cot \delta_0 = -\frac{1}{a_0} + \frac{1}{2}r_{\text{eff}}k^2 + O(k^4)$, where a_0 and r_{eff} are the scattering length and the effective range, respectively. The results are

$$\begin{aligned} a_0 &= 1.57(0.08)^{(+0.12)}_{(-0.04)} \text{ fm}, \\ r_{\text{eff}} &= 0.57(0.02)^{(+0.01)}_{(-0.00)} \text{ fm}. \end{aligned} \quad (4)$$

The central values and the statistical errors in the first parentheses are obtained at $t/a = 26$, while the systematic errors in the last parentheses are estimated from the values at $t/a = 25, 26$ and 27, which originates from the inelastic states and the higher order terms of the derivative expansion.

The binding energy B and the root-mean-square distance $\sqrt{\langle r^2 \rangle}$ of the bound $\Omega_{ccc}\Omega_{ccc}$ state are obtained from the potential $V(r)$ as

$$\begin{aligned} B &= 5.68(0.77)^{(+0.46)}_{(-1.02)} \text{ MeV}, \\ \sqrt{\langle r^2 \rangle} &= 1.13(0.06)^{(+0.08)}_{(-0.03)} \text{ fm}. \end{aligned} \quad (5)$$

These results are consistent with the general formula for loosely bound states [24, 37] with scattering parameters a_0 and r_{eff} : $B = 1/(m_{\Omega_{ccc}} r_{\text{eff}}^2)(1 - \sqrt{1 - (2r_{\text{eff}}/a_0)})^2 \simeq 5.7$ MeV and $\sqrt{\langle r^2 \rangle} = a_0/\sqrt{2} \simeq 1.1$ fm.

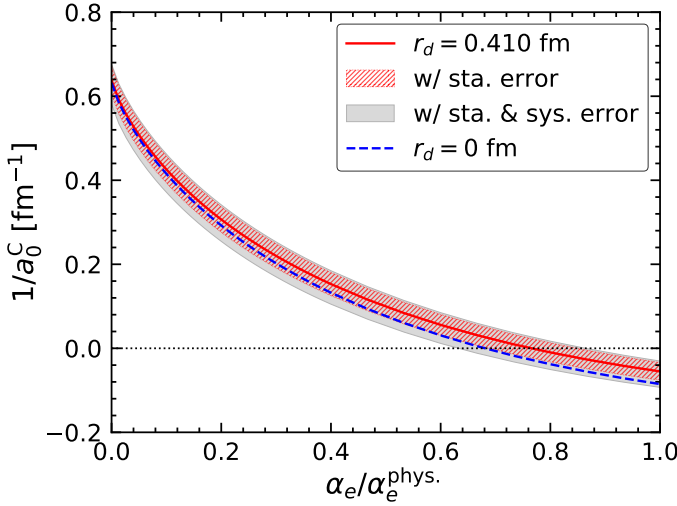


FIG. 3. (Color online). The inverse of the scattering length $1/a_0^C$ as a function of $\alpha_e/\alpha_e^{\text{phys.}}$. The red solid line is the central values for $r_d = 0.410$ fm. The statistical errors are shown by the inner band (red), while the outer band (gray) corresponds to the statistical and systematic errors added in quadrature. The blue dashed line corresponds to the central values for $r_d = 0$ fm.

Since the binding energy and the size of the bound state from the strong interaction are not large, we need to take into account the Coulomb repulsion $V^{\text{Coulomb}}(r)$ between Ω_{ccc}^{++} s with finite spatial size. For this purpose, we consider the dipole form factor for Ω_{ccc}^{++} according to the LQCD study on the charge distribution of heavy baryons [18]: In the coordinate space, it corresponds to an exponential charge distribution $\rho(r) = 12\sqrt{6}/(\pi r_d^3)e^{-2\sqrt{6}r/r_d}$, where the charge radius $r_d = \sqrt{\langle r^2 \rangle_{\text{charge}}}$ of Ω_{ccc}^{++} is taken to be $r_d = 0.410(6)$ fm [18]. Then, we have

$$V^{\text{Coulomb}}(r) = \alpha_e \iint d^3r_1 d^3r_2 \frac{\rho(r_1)\rho(|\vec{r}_2 - \vec{r}_1|)}{|\vec{r}_1 - \vec{r}_2|} = \frac{4\alpha_e}{r} F(x), \quad (6)$$

where $x = 2\sqrt{6}r/r_d$ and $F(x) = 1 - e^{-x}(1 + \frac{11}{16}x + \frac{3}{16}x^2 + \frac{1}{48}x^3)$. The effective range expansion with Coulomb repulsion is written as

$$k [C_\eta^2 \cot \delta_0^C(k) + 2\eta h(\eta)] = -\frac{1}{a_0^C} + \frac{1}{2}r_{\text{eff}}^C k^2 + O(k^4), \quad (7)$$

where $\delta_0^C(k)$ is the phase shift in the presence of Coulomb repulsion, $C_\eta^2 = \frac{2\pi\eta}{e^{2\pi\eta}-1}$, $\eta = 2\alpha_e m_{\Omega_{ccc}}/k$, $h(\eta) = \text{Re}[\Psi(i\eta)] - \ln(\eta)$, and Ψ is the digamma function [38]. To see the effect of the Coulomb repulsion, we vary α_e from zero to the physical value $\alpha_e^{\text{phys.}} = 1/137.036$ below. Note that the systematic errors originated from the uncertainty in r_d are found to be much smaller than the statistical errors and are neglected.

In Fig. 3, we show the inverse of scattering length $1/a_0^C$ under the change of $\alpha_e/\alpha_e^{\text{phys.}}$ from 0 to 1. Due

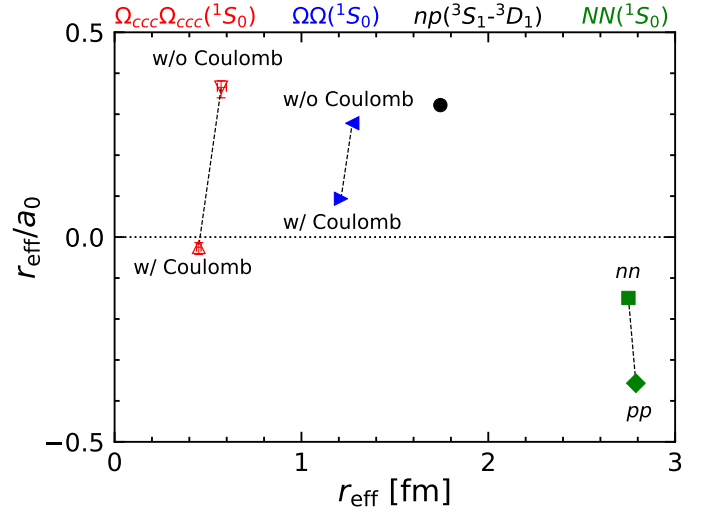


FIG. 4. (Color online). The dimensionless ratio of the effective range r_{eff} and the scattering length a_0 as a function of r_{eff} . The red up(down)-pointing triangle and the blue right(left)-pointing triangle correspond to $\Omega_{ccc}\Omega_{ccc}$ system and $\Omega\Omega$ system in the 1S_0 channel with(without) the Coulomb repulsion respectively. The black circle represents NN system in the 3S_1 - 3D_1 channel. The green square (nn) and diamond (pp) correspond to NN system in the 1S_0 channel. The error bars for $\Omega_{ccc}\Omega_{ccc}$ are the quadrature of the statistical and systematic errors in Eqs. (4) and (8).

to the large cancellation between the attractive strong interaction and the Coulomb repulsion, the result at $\alpha_e/\alpha_e^{\text{phys.}} = 1$ is located very close to unitarity with a large scattering length

$$\begin{aligned} a_0^C &= -19(7)_{(-6)}^{(+7)} \text{ fm}, \\ r_{\text{eff}}^C &= 0.45(0.01)_{(-0.00)}^{(+0.01)} \text{ fm}. \end{aligned} \quad (8)$$

The ratio $r_{\text{eff}}^C/a_0^C = -0.024(0.010)_{(-0.014)}^{(+0.006)}$ is considerably smaller in magnitude than that of the dineutron (-0.149).

In Fig. 4, we plot the dimensionless ratio r_{eff}/a_0 as a function of r_{eff} for $\Omega_{ccc}^{++}\Omega_{ccc}^{++}(^1S_0)$ and $\Omega^-\Omega^-(^1S_0)$ with (without) Coulomb repulsion together with the experimental values for $NN(^3S_1$ - $^3D_1)$ [39] and $NN(^1S_0)$ [40, 41]. Note that we consider the Coulomb repulsion in $\Omega^-\Omega^-(^1S_0)$ with the charge radius $r_d = 0.57$ fm for Ω^- [18].³ Among all those dibaryon systems, $\Omega_{ccc}^{++}\Omega_{ccc}^{++}(^1S_0)$ is the closest to unitarity.

Finally, we briefly discuss other possible systematic errors in this work: (i) The finite cutoff effect is $\mathcal{O}(\alpha_s^2 a \Lambda_{\text{QCD}}, (a \Lambda_{\text{QCD}})^2)$ thanks to the RHQ action for the charm quark and the non-perturbative $O(a)$ improvement for light (u, d, s) quarks, and thus amounts to be

³ In Ref.[10], Ω^- was assumed to be point-like in charge distribution, which overestimates the repulsion and increases the scattering length by 1 fm.

$\mathcal{O}(1)\%$. (ii) In the vacuum polarization, light quark masses are slightly heavier than the physical ones and charm quark loop is neglected. The former effect is expected to be small since light quarks are rather irrelevant for $\Omega_{ccc}\Omega_{ccc}$ system. In fact, the range of the $\Omega_{ccc}\Omega_{ccc}$ potential is found to be shorter than 1 fm. The latter effect is suppressed due to the heavy charm quark mass, and is typically $\mathcal{O}(1)\%$ [42]. These estimates for (i) and (ii) are also in line with the observation that our value of $m_{\Omega_{ccc}}$ is consistent with that in the literature or has deviation of $\sim 1\%$ at most, where we refer to LQCD studies by (2+1)-flavor at the physical point with finite a [34], (2+1)-flavor with chiral and continuum extrapolation [43] and (2+1+1)-flavor with chiral and continuum extrapolation [44, 45]. In the future, these systematic errors will be evaluated explicitly.

Summary and discussions.— In this Letter, we presented a first investigation on the scattering properties of the $\Omega_{ccc}\Omega_{ccc}$ on the basis of the (2+1)-flavor lattice QCD simulations with physical charm mass and nearly physical light quark masses. The potential for $\Omega_{ccc}\Omega_{ccc}(^1S_0)$ obtained by the time-dependent HAL QCD method without the Coulomb interaction shows a weak repulsion at short distance surrounded by a relatively strong attractive well, which leads to a most charming ($C = 6$) dibaryon with the binding energy $B \simeq 5.7$ MeV and the size $\sqrt{\langle r^2 \rangle} \simeq 1.1$ fm. By taking into account the Coulomb repulsion between Ω_{ccc}^{++} s with their charge form factor obtained from LQCD, the $\Omega_{ccc}^{++}\Omega_{ccc}^{++}(^1S_0)$ system turns into the unitary region with $r_{\text{eff}}^C/a_0^C \simeq -0.024$. This provides good information toward the understanding of the interaction between heavy baryons. It is an interesting future work to study $\Omega_{bbb}^-\Omega_{bbb}^-(^1S_0)$ for revealing the quark mass dependence of the scattering parameters. Finally, our results may further stimulate the future experimental activities to measure pair-momentum correlations of heavy baryons in high energy pp , pA and AA collisions [8, 14].

Acknowledgments.— We thank the members of HAL QCD Collaboration for technical supports and stimulating discussions. We thank Yusuke Namekawa for providing the RHQ parameters. We thank members of PACS Collaboration for the gauge configuration generation conducted on the K computer at RIKEN. The lattice QCD measurements have been performed on HOKUSAI supercomputers at RIKEN. This work was partially supported by HPCI System Research Project (hp120281, hp130023, hp140209, hp150223, hp150262, hp160211, hp170230, hp170170, hp180117, hp190103). We thank ILDG/JLDG [46], which serves as an essential infrastructure in this study. We thank the authors of cuLGT code [47] for the gauge fixing. We thank Tatsuaki Aoyama, Haozhao Liang, Shuangquan Zhang and Pengwei Zhao for helpful discussions. Y.L., H.T. and J.M. were partially supported by the National Key R&D

Program of China (Contracts No. 2017YFE0116700 and No. 2018YFA0404400) and the National Natural Science Foundation of China (NSFC) under Grants No. 11935003, No. 11975031, No. 11875075, and No. 12070131001. This work was partially supported by JSPS Grant (No. JP18H05236, JP16H03978, JP19K03879, JP18H05407) and MOST-RIKEN Joint Project “Ab initio investigation in nuclear physics”, “Priority Issue on Post-K computer” (Elucidation of the Fundamental Laws and Evolution of the Universe), “Program for Promoting Researches on the Supercomputer Fugaku” (Simulation for basic science: from fundamental laws of particles to creation of nuclei) and Joint Institute for Computational Fundamental Science (JICFuS).

* Y. L. and H. T. contributed equally to this Letter and should be considered as co-first authors.

helvetia@pku.edu.cn

† Corresponding author.

tongh16@pku.edu.cn

- [1] E. Epelbaum, H.-W. Hammer, and U.-G. Meißner, *Rev. Mod. Phys.* **81**, 1773 (2009).
- [2] J. Meng, *Relativistic Density Functional for Nuclear Structure* (World Scientific, Singapore, 2016).
- [3] S. Shen, H. Liang, W. H. Long, J. Meng, and P. Ring, *Progress in Particle and Nuclear Physics* **109**, 103713 (2019).
- [4] C. Drischler, W. Haxton, K. McElvain, E. Mereghetti, A. Nicholson, P. Vranas, and A. Walker-Loud (2019) arXiv:1910.07961 [nucl-th].
- [5] H. Tong, P. Zhao, and J. Meng, *Phys. Rev. C* **101**, 035802 (2020).
- [6] H. Clement, *Progress in Particle and Nuclear Physics* **93**, 195 (2017).
- [7] A. Gal, *Acta Phys. Polon. B* **47**, 471 (2016), arXiv:1511.06605 [nucl-th].
- [8] S. Cho, T. Hyodo, D. Jido, C. M. Ko, S. H. Lee, S. Maeda, K. Miyahara, K. Morita, M. Nielsen, A. Ohnishi, T. Sekihara, T. Song, S. Yasui, and K. Yazaki, *Progress in Particle and Nuclear Physics* **95**, 279 (2017).
- [9] T. Iritani, S. Aoki, T. Doi, F. Etminan, S. Gongyo, T. Hatsuda, Y. Ikeda, T. Inoue, N. Ishii, T. Miyamoto, and K. Sasaki, *Physics Letters B* **792**, 284 (2019).
- [10] S. Gongyo, K. Sasaki, S. Aoki, T. Doi, T. Hatsuda, Y. Ikeda, T. Inoue, T. Iritani, N. Ishii, T. Miyamoto, and H. Nemura (HAL QCD Collaboration), *Phys. Rev. Lett.* **120**, 212001 (2018).
- [11] S. Aoki and T. Doi, *Frontiers in Physics* **8**, 307 (2020).
- [12] K. Morita, S. Gongyo, T. Hatsuda, T. Hyodo, Y. Kamiya, and A. Ohnishi, *Phys. Rev. C* **101**, 015201 (2020), arXiv:1908.05414 [nucl-th].
- [13] S. Acharya *et al.* (ALICE Collaboration), *Nature* **588**, 232 (2020).
- [14] L. Fabbietti, V. M. Sarti, and O. V. Doce, (2020), arXiv:2012.09806 [nucl-ex].
- [15] J. Bjorken, *AIP Conf. Proc.* **132**, 390 (1985).
- [16] R. Aaij *et al.* (LHCb Collaboration), *Phys. Rev. Lett.* **118**, 182001 (2017).

- [17] R. Aaij *et al.* (LHCb Collaboration), Phys. Rev. Lett. **119**, 112001 (2017).
- [18] K. U. Can, G. Erkol, M. Oka, and T. T. Takahashi, Phys. Rev. D **92**, 114515 (2015).
- [19] H. Huang, J. Ping, X. Zhu, and F. Wang, arXiv:2011.00513 [hep-ph].
- [20] P. Junnarkar and N. Mathur, Phys. Rev. Lett. **123**, 162003 (2019).
- [21] J.-M. Richard, A. Valcarce, and J. Vijande, Phys. Rev. Lett. **124**, 212001 (2020).
- [22] N. Ishii, S. Aoki, and T. Hatsuda, Phys. Rev. Lett. **99**, 022001 (2007).
- [23] N. Ishii, S. Aoki, T. Doi, T. Hatsuda, Y. Ikeda, T. Inoue, K. Murano, H. Nemura, and K. Sasaki (HAL QCD Collaboration), Physics Letters B **712**, 437 (2012).
- [24] E. Braaten and H.-W. Hammer, Physics Reports **428**, 259 (2006).
- [25] C. Chin, R. Grimm, P. Julienne, and E. Tiesinga, Rev. Mod. Phys. **82**, 1225 (2010).
- [26] G. P. Lepage, in *From Actions to Answers: Proceedings of the TASI 1989*, edited by T. Degrand and D. Toussaint (World Scientific, Singapore, 1990).
- [27] T. Iritani, S. Aoki, T. Doi, T. Hatsuda, Y. Ikeda, T. Inoue, N. Ishii, H. Nemura, and K. Sasaki (HAL QCD), JHEP **03**, 007 (2019), arXiv:1812.08539 [hep-lat].
- [28] M. Yamada, K. Sasaki, S. Aoki, T. Doi, T. Hatsuda, Y. Ikeda, T. Inoue, N. Ishii, K. Murano, and H. Nemura (HAL QCD), PTEP **2015**, 071B01 (2015), arXiv:1503.03189 [hep-lat].
- [29] K.-I. Ishikawa, N. Ishizuka, Y. Kuramashi, Y. Nakamura, Y. Namekawa, Y. Taniguchi, N. Ukita, T. Yamazaki, and T. Yoshie (PACS), *Proc. Sci. LATTICE2015*, 075 (2016), arXiv:1511.09222 [hep-lat].
- [30] S. Aoki, Y. Kuramashi, and S.-i. Tominaga, Prog. Theor. Phys. **109**, 383 (2003), arXiv:hep-lat/0107009.
- [31] Y. Namekawa (PACS), *Proc. Sci. LATTICE2016*, 125 (2017).
- [32] http://bridge.kek.jp/Lattice-code/index_e.html.
- [33] T. Doi and M. G. Endres, Computer Physics Communications **184**, 117 (2013).
- [34] Y. Namekawa, S. Aoki, K.-I. Ishikawa, N. Ishizuka, K. Kanaya, Y. Kuramashi, M. Okawa, Y. Taniguchi, A. Ukawa, N. Ukita, and T. Yoshié (PACS-CS Collaboration), Phys. Rev. D **87**, 094512 (2013).
- [35] T. Doi *et al.*, *Proc. Sci. LATTICE2016*, 110 (2017), arXiv:1702.01600 [hep-lat].
- [36] M. Oka, K. Shimizu, and K. Yazaki, Nuclear Physics A **464**, 700 (1987).
- [37] P. Naidon and S. Endo, Reports on Progress in Physics **80**, 056001 (2017).
- [38] P. G. Burke, *R-Matrix Theory of Atomic Collisions* (Springer-Verlag, Berlin, 2011).
- [39] R. W. Hackenburg, Phys. Rev. C **73**, 044002 (2006).
- [40] J. R. Bergervoet, P. C. van Campen, W. A. van der Sanden, and J. J. de Swart, Phys. Rev. C **38**, 15 (1988).
- [41] I. Slaus, Y. Akaishi, and H. Tanaka, Physics Reports **173**, 257 (1989).
- [42] S. Aoki *et al.* (Flavour Lattice Averaging Group), Eur. Phys. J. C **80**, 113 (2020), arXiv:1902.08191 [hep-lat].
- [43] Z. S. Brown, W. Detmold, S. Meinel, and K. Orginos, Phys. Rev. D **90**, 094507 (2014).
- [44] R. A. Briceño, H.-W. Lin, and D. R. Bolton, Phys. Rev. D **86**, 094504 (2012).
- [45] C. Alexandrou, V. Drach, K. Jansen, C. Kallidonis, and G. Koutsou, Phys. Rev. D **90**, 074501 (2014).
- [46] <http://www.lqcd.org/ildg> and <http://www.jldg.org>.
- [47] M. Schrock and H. Vogt, Computer Physics Communications **184**, 1907 (2013).